Appendix 7. Conduit Flow Process Updates and Upgrades (CFP2)

The conduit flow process allows for the coupled simulation of pipes or other preferential flow paths within an aquifer (that is, a discrete-continuum model). The aquifer volume is represented by a porous medium (that is, matrix) and preferential flow paths (for example, conduits or mine adits). Preferential flow paths are simulated as linear pathways in the aquifer. In this version of conduit flow process (CFP2), several modifications and increased capabilities were developed for conduit boundary conditions, time-series analysis (TSA) and output, conduit storage, and length-dependent exchange. The newly added boundary conditions and conduit storage features available in CFP2 include the following:

- Time series as input files (for example, for boundaries—important because of highly conductive pipes).
- Additional mixed boundary conditions (Cauchy, combined Dirichlet-Neumann).
- Additional direct storage for discrete pipe structures simulated as Conduit Accessible Drainable Storage (CADS).
- Water release by dewatering discrete elements through partially filled pipe storage.

This appendix summarizes the conceptual framework of each of these new features in the second version of the Conduit Flow Process (CFP2). Instructions to implement the new features are presented in appendix 8.

Time-Dependent Boundary Conditions

Flow through karst conduits can respond to changed boundary conditions very quickly and sensitively because of the high conductivity. Consequently, transient models can require time-dependent (TD) boundary conditions, such as pumping rates (well boundary conditions) or river stages (Cauchy boundary conditions). As originally implemented in CFP1 (Shoemaker and others, 2008), time-dependent input was applied by dividing the model time step into several periods. For karst systems, however, this can result in inefficient input files for a number of such periods. CFP2 Mode 1 was modified to read time-dependent data from an external file and to compute boundary conditions for each model time step to account for time-dependent boundary conditions in one model stress period. This functionality is useful for various boundary conditions:

- Fixed head boundary
- Fixed head limited flow boundary (FHLQ)
- Well boundary (QWELL)
- Cauchy boundary

The approach to linear interpolation of temporally varying boundary conditions across model time-steps is as follows:

$$x_t = \frac{t - t_p}{t_n - t_p}\left(x_n - x_p\right) + x_p \tag{7.1}$$

where

x_t is the interpolated boundary condition value at time, t;
t_p is the time of previous data entry;
t_n is the time of next data entry;
x_p is the previous data entry boundary condition value; and
x_n is the next data entry boundary condition value.

Measured data from a large-scale pumping test (Maréchal and others, 2008), introduced in the "Conduit-Associated Drainable Storage" section, are used to demonstrate the functionality enabled by TD boundary conditions. Hence, measured pumping rates are treated as time-dependent data having a resolution of 3,600 seconds. Results are presented in figure 7.1 and show that (1) variable pumping rates are correctly considered by the numerical model using TD data and (2) relatively small variability in pumping can cause large variation in well drawdown.

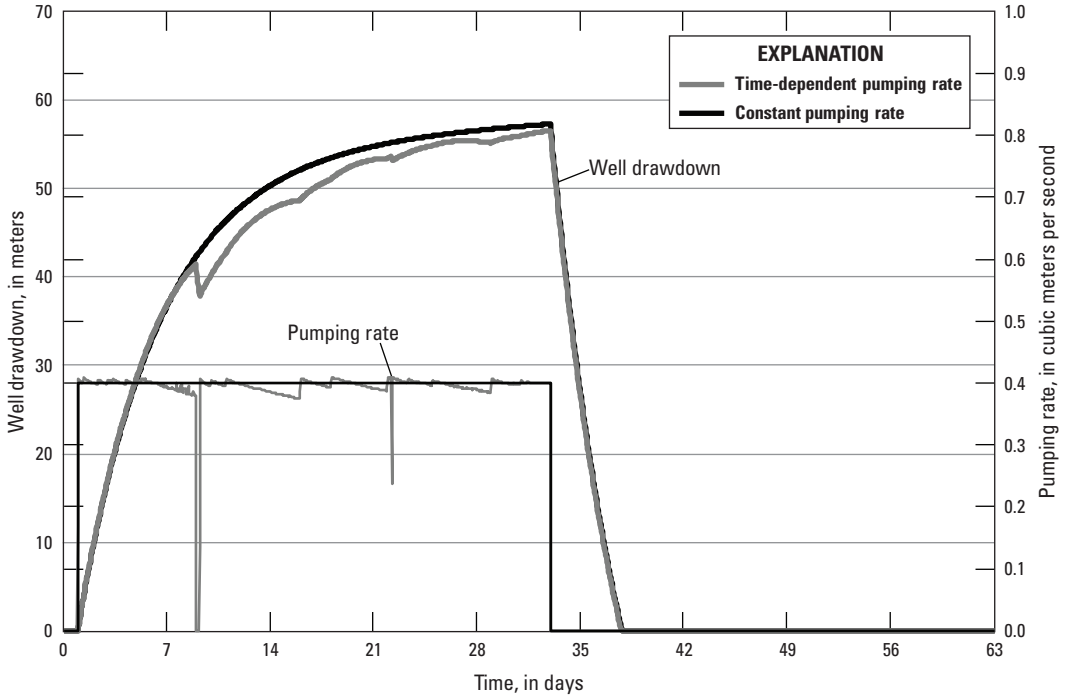

Figure 7.1. Simulation using CFP2 with time-dependent boundary conditions (pumping rate from Maréchal and others, 2008).

Fixed Head Limited Flow (FHLQ) Boundary Condition

A conduit with fixed head boundary condition can strongly affect inflow or outflow of the highly permeable conduit network. For example, water extraction from a network of conduits with sufficiently large diameters almost always results in water inflow through the fixed head boundary. Often, these exchange rates are limited by hydrologic properties of the porous matrix (for example, hydraulic conductivity). Therefore, it may be useful for some simulations to constrain the flow rate to the conduit network across a fixed head boundary and limit exchanges between the conduit network and the porous matrix. The FHLQ boundary condition is intended to limit inflow or outflow at constant head boundaries. If a user-defined limiting flow rate (threshold) is exceeded, the boundary condition switches from a fixed head to a constant-flow boundary, which results in variable head (Bauer and others, 2005):

$$FHLQ = \begin{Bmatrix} h = H, & Q \le Q_L \\ Q = Q_L, & \text{else} \end{Bmatrix} \sqrt{a^2 + b^2} \tag{7.2}$$

where

h is the head at the conduit node,
H is the fixed head value,
Q is the discharge at the boundary (negative values denote outflow), and
Q_L is the limiting flow rate (LQ).

This boundary condition was not included in the previous version of the conduit flow process (CFP1). The fixed head limited flow boundary condition existed in the discrete continuum model Carbonate Aquifer Void Evolution (CAVE; Liedl and others, 2003). The CAVE model provided the theoretical basis for CFP Mode 1. The FHLQ boundary condition has been added to CFP2 for Mode 1.

Well Boundary Condition

This boundary condition can be used to apply pumping to a conduit node. Prior to CFP2, this was done by using the recharge (RCH) package along with direct recharge percentage (CRCH). This update allows recharge to be apportioned to a conduit and extracted from the conduit to improve accounting of pumpage by conduits in the budget files. This is a newly developed feature of CFP2 to use with Mode 1.

Cauchy Boundary Condition

The Cauchy boundary condition (CYLQ) can be used to provide head-dependent flow to a node, like the River GHB package in MODFLOW. Flow at the Cauchy boundary, Q_{cy}, is computed as follows:

$$Q_{cy} = c_{cy}\left(h - h_{cy}\right) \tag{7.3}$$

where

c_{cy} is the Cauchy conductance, where 0 is less than c_{cy}, which is less than infinity, and is normal to the boundary;
h is the hydraulic head in the conduit; and
h_{cy} is the Cauchy head.

Negative values for Q_{cy} denote inflow into the conduit system. Additionally, inflow can be limited by a CYLQ condition, as for the FHLQ boundary described in this appendix (see the "Fixed Head Limited Flow (FHLQ) Boundary Condition" section).

$$CYLQ = \begin{cases} Q = Q_{cy}, & Q \le Q_L \\ Q = Q_L, & \text{else} \end{cases} \tag{7.4}$$

where

Q_L is the limiting flow rate (LQ).

Limited Head Boundary Condition (LH)

This boundary condition can be used to provide a limitation for the node-head, for example, to represent a flooded sinkhole for which the limited head is equivalent to the ground surface (fig. 7.2). This is newly developed feature of CFP2 for use with Mode 1. The hydraulic head for the limited head (LH) boundary condition is computed as follows:

$$h_{LH} = \begin{cases} h, & h \le H_{LH} \\ h = H_{LH}, & \text{else} \end{cases} \tag{7.5}$$

where

h is the computed hydraulic head
h_{LH} is the head at the limited head boundary node, and
H_{LH} is the limited head.

Note that LH boundaries only apply to groundwater-outflow situations and, therefore, are equivalent to FHLQ boundaries where LQ = 0, but they allow for improved representation of water flow in water budgets.

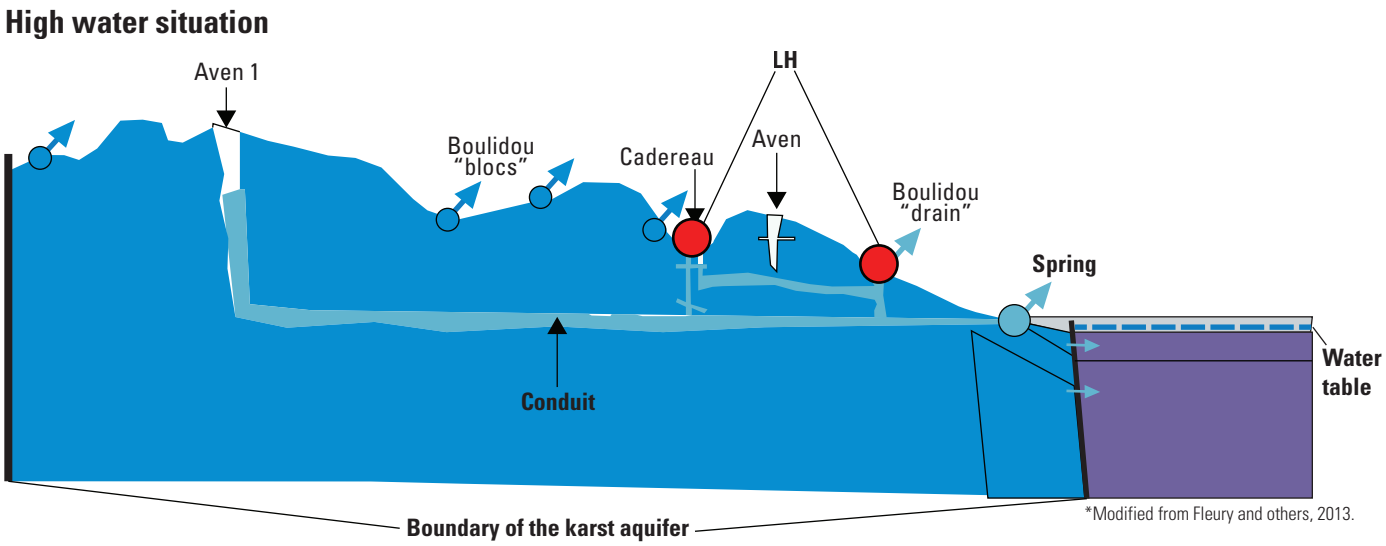

Figure 7.2. Conceptual diagram of the application of the limited head (LH) boundary (from Fleury and others, 2013).

Conduit-Associated Drainable Storage (CADS)

Karst aquifers can be conceptualized in several ways. One common way is to represent the karst system by highly permeable conduits embedded in a low permeability matrix continuum (for example, Király, 1997). Others describe karst systems as pipes draining associated karstic storage, and the matrix storage is negligible (for example, Mangin, 1994). Depending on the investigated karst system, as well as the considered time scale, three karst features can predominate:

- Pipes
- Drainable storage (like caves, large fractures, and fissures)
- The matrix continuum.

An example is the large-scale pumping test by Maréchal and others (2008), which demonstrates the drawdown reaction of conduit and matrix heads in response to long-term pumping. Results from this test provide arguments for the presence and importance of karst conduits, associated karstic storage (responsible for conduit drawdown), and matrix storage (responsible for matrix drawdown).

To consider drainable storage in CFP2 Mode 1, the CADS package (conduit-associated drainable storage) was developed. The CADS package simulates an independent storage zone with an independently calculated hydraulic head. The CADS storage is assumed to be in direct hydraulic contact with draining conduits:

$$h_{conduit} = h_{CADS} \tag{7.6}$$

where

$h_{conduit}$ is the head at the conduit node, and
h_{CADS} is the CADS head, which is also related to the conduit node.

It is assumed that water released from the CADS due to head variations immediately enters the conduit, resulting in additional discharge. The resulting flow rate from and to the CADS, Q_{CADS}, is as follows:

$$Q_{CADS} = \frac{V_t - V_{t-\Delta t}}{\Delta t} \tag{7.7}$$

where

V_t is the volume of the CADS at time t, and
Δt is the time step size.

Finally, the volume of the CADS, V_{CADS}, is computed:

$$V_{CADS} = L_{CADS} W_{CADS} \left(h_{CADS} - z_{bottom} \right); h_{CADS} > z_{bottom} \tag{7.8}$$

where

L_{CADS} is the length, which is assumed to equal the length of the conduit;
W_{CADS} is the width of the CAD storage; and
z_{bottom} is the conduit base elevation.

The CADS package was newly developed for CFP2 for use with Mode 1. Figure 7.3 shows the conceptual implementation of CADS for a karst catchment.

Potential application of the CADS functionality in CFP2 Mode1 is demonstrated here by simulating the large-scale pumping test by Maréchal and others (2008) in a very preliminary, simplified manner (intended only to demonstrate CADS functionality). Measured data used to develop this demonstration model are available in Maréchal and others (2008); a conceptual sketch of the demonstration model is shown in figure 7.4. Parameters used are presented in table 7.1. Results of computed and measured drawdown at the conduit and in the matrix are presented in figure 7.5 and resulting computed flows for several compartments of the model are listed in table 7.2.

Simulated drawdown and flow terms compared reasonably well with the measured data from Maréchal and others (2008). This comparison illustrates the new functionality of the CADS function in CFP2 Mode 1 and is for demonstration purposes only. This demonstration, which was not rigorously calibrated, shows the potential applicability of CFP MODE 1 with CADS and the FHLQ boundary condition to represent long-term pumping from karst water resources.

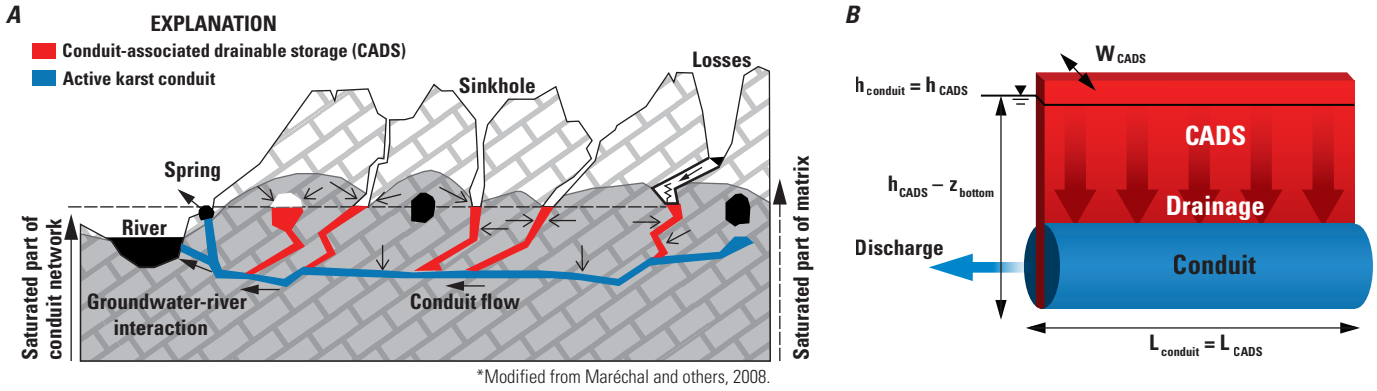

Figure 7.3. Conceptual implementation of CADS for a karst catchment as *A*, conceptual cross section (diagram modified from Maréchal and others, 2008) and *B*, simplification to illustrate terms used in equation 7.8.

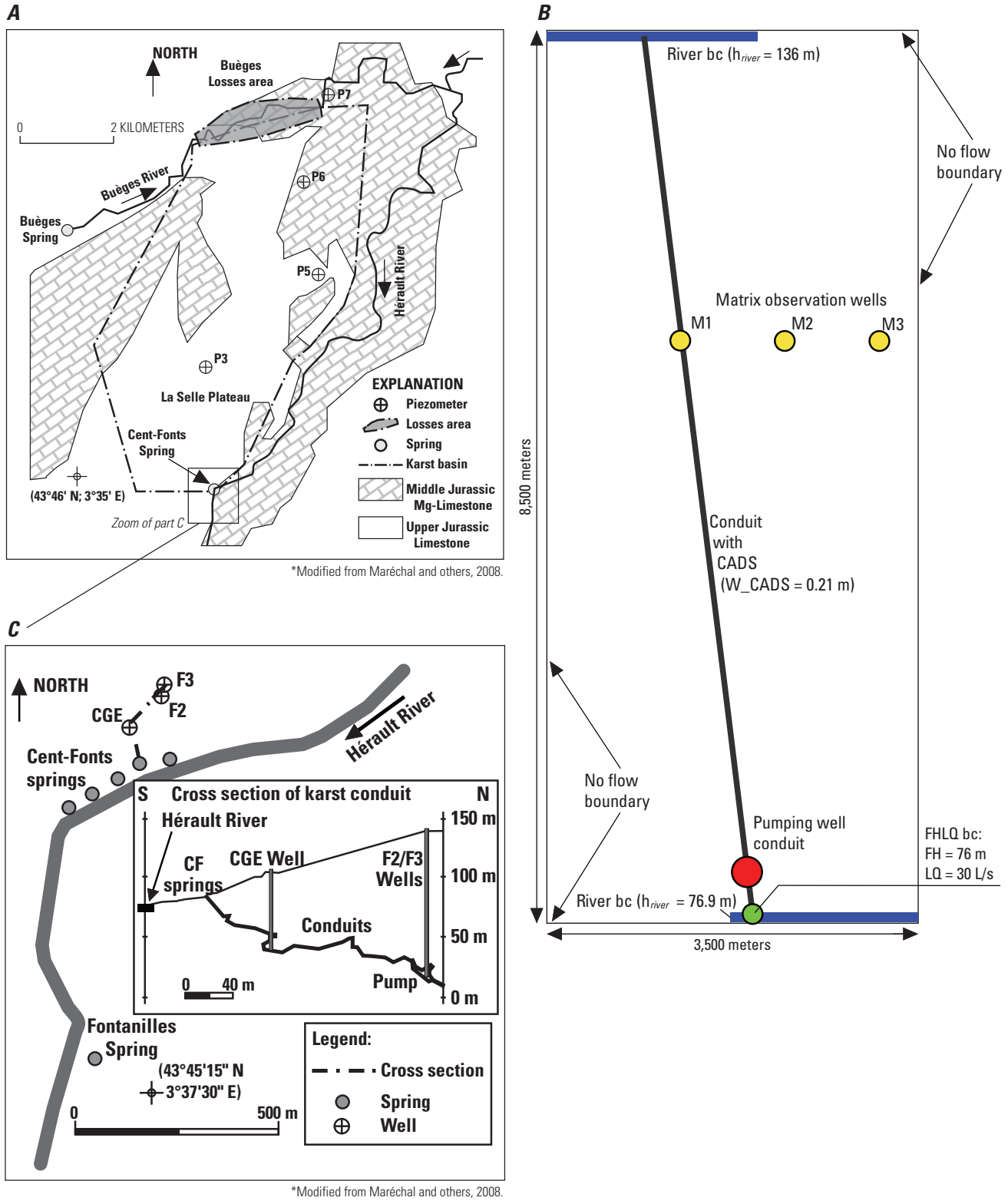

Figure 7.4. Map and diagram of the model demonstration of a large-scale pumping test: *A*, area of catchment where test was done and location of pumping well F3 and Cent-Fonts spring inside the inset black box (map from Maréchal and others, 2008); *B*, conceptual representation in planimetric view of the modeled scenario of the test showing the river boundary condition (River bc) where the head in the river (h_{river}) is specified as meters above sea level (masl), and fixed head limited flow boundary condition (FHLQ bc) where the fixed head (FH) is 76 masl and the limited flux (LQ) is specified as 30 liters per second (L/s); and *C*, Cent-Fonts spring area showing Cent-Fonts springs, Fontanilles Spring, Hérault River; CGE, F2, and F3 wells, and cross section of karst conduits.

Table 7.1. Parameters used for the large-scale pumping test model comparing CFP2 MODE 1 with Conduit Accessible Drainable Storage (CADS) to the data from Maréchal and others (2008).

[a^{-1}, per annum; h, hours; km, kilometers; km^2, square kilometers; m, meter; m^2, square meters; mm, millimeters; s^{-1}, per second; P1, P2, and P3 refer to stress period time step length with recharge rates defined by recharge rates R1, R2, and R3, respectively; —, no data]

Parameter	Data from Maréchal and others (2008)	Parameter for CFP MODE 1/CADS
Matrix continuum		
Area	30 km^2	3.5 km × 8.5 km = 29.75 km^2; 35 x 85 cells with $\Delta x = \Delta y$ = 100 m
top/bottom	—	250 m / –150 m
$T¬m$	1.6×10^{-5} m^2s^{-1}	—
K_m	—	9.0×10^{-6} ms^{-1}
S_m	0.007	0.007 (S_S = 0.00001)
Conduit		
Length	—	~ 9.1 km
Diameter	—	3.5 m
Roughness	—	0.01 m
S_c (free surface area of dewatering conduit network)	1,900 m^2	$S_C \sim A_{CADS}$; W_{CADS} = 1,900 m^2 / 9,100 m = 0.21 m
pipe conductance (α)	—	4.5×10^{-5} m^2s^{-1}
time discretization	—	P1: 1 day initialization (steady state)
		P2: 32 days pumping (transient, dt = 1h)
		P3: 32 days recovery (transient, dt = 1h)
diffuse recharge	—	R1: $6.3376 \times 10^{-9}¬$ ms^{-1} (200 mm a^{-1})
		R2: $6.3376 \times 10^{-9}¬$ ms^{-1}
		R3: $6.3376 \times 10^{-9}¬$ ms^{-1}

Table 7.2. Comparison between flow rates from Maréchal and others (2008) and the CFP2 MODE 1 with Conduit Accessible Drainable Storage (CADS) simulated results.

[bc, boundary condtion; CADS Conduit Accessible Drainable Storage; FHLQ, Fixed Head Limited Flow; m, meter; m^3, cubic meters; s^{-1}, per second]

Flow compartment	Data from Maréchal and others (2008)	Computed by CFP MODE 1/CADS
Spring discharge (steady state)	0.250 m^3s^{-1}	0.148 m^3s^{-1}
Inflow Hérault (river bc, at the karst spring)	0.030 m^3s^{-1}	0.030 m^3s^{-1} (FHLQ bc)
Bueges losses (river bc, at the origin of the conduit)	0.010 m^3s^{-1}	0.005 m^3s^{-1} (steady state) up to 0.010 m^3s^{-1} (during pumping)
Matrix water inflow to conduits	0.240 m^3s^{-1}	0.147 m^3s^{-1} (steady state) up to 0.367 m^3s^{-1} (during pumping)

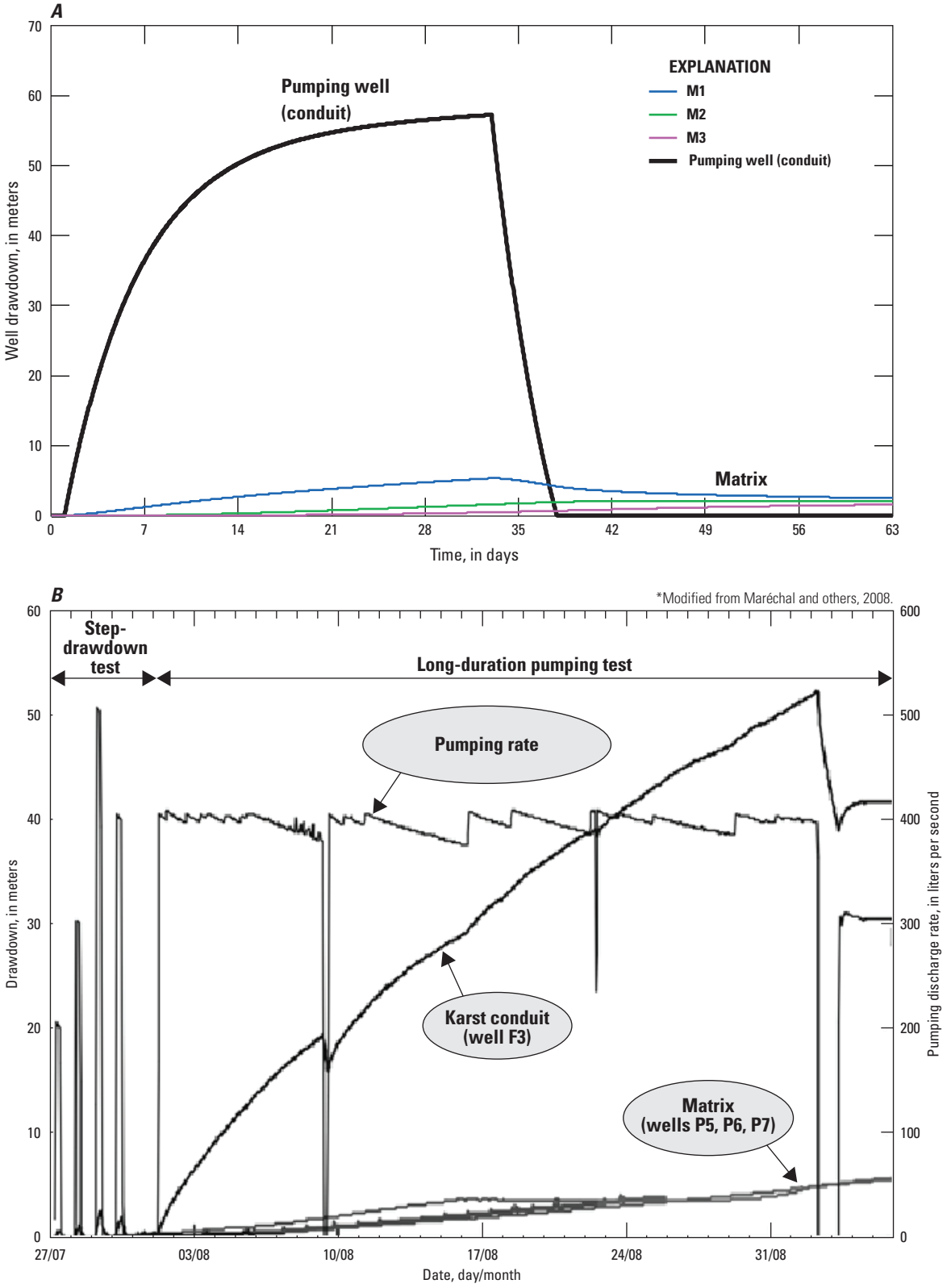

Figure 7.5. Drawdown results from a large-scale pumping test: *A*, computed drawdown for matrix wells M1, M2 and M3 and conduit shown in figure 7.4*B*; and *B*, measured drawdown from field test (from Maréchal and others, 2008).

Multi-Layer CADS (CADSML)

This new option allows a CADS volume to vary as a function of elevation. Hence, CADS width W_{CADS} is no longer uniform with depth. This allows Multi-Layer CADS (CADSML) users to limit CADS to specific areas (that is, restrict CADS to below the ground surface or to layers with a free water table inside CADS storage).

The numerical approach to implement CADSML is like that of partially filled pipe storage (PFPS), which is presented in a separate section of this appendix (equations 7–9 and 7–10). The concept of CADSML is illustrated in figure 7.6. Although the system shown in figure 7.6 has only two layers with non-zero width, CADSML can account for up to four different CADS layers ($z1$ / $W_{CADS}1$ … $z4$ / $W_{CADS}4$).

The numerical solution of multilayer CADS can result in oscillations, which is likely for situations with rapidly varying boundary conditions (for example, reduction or stopping of pumping) and subsequent conduit head change along flowpaths where values of W_{CADS} vary notably. The CFP2 considers oscillations by analyzing five successive iterations and, if there are oscillations, changes the relaxation parameter (line 20 of the CFP2 input file, Shoemaker and others, 2008, p. 27) to 5 percent of the initial value until the next iteration loop.

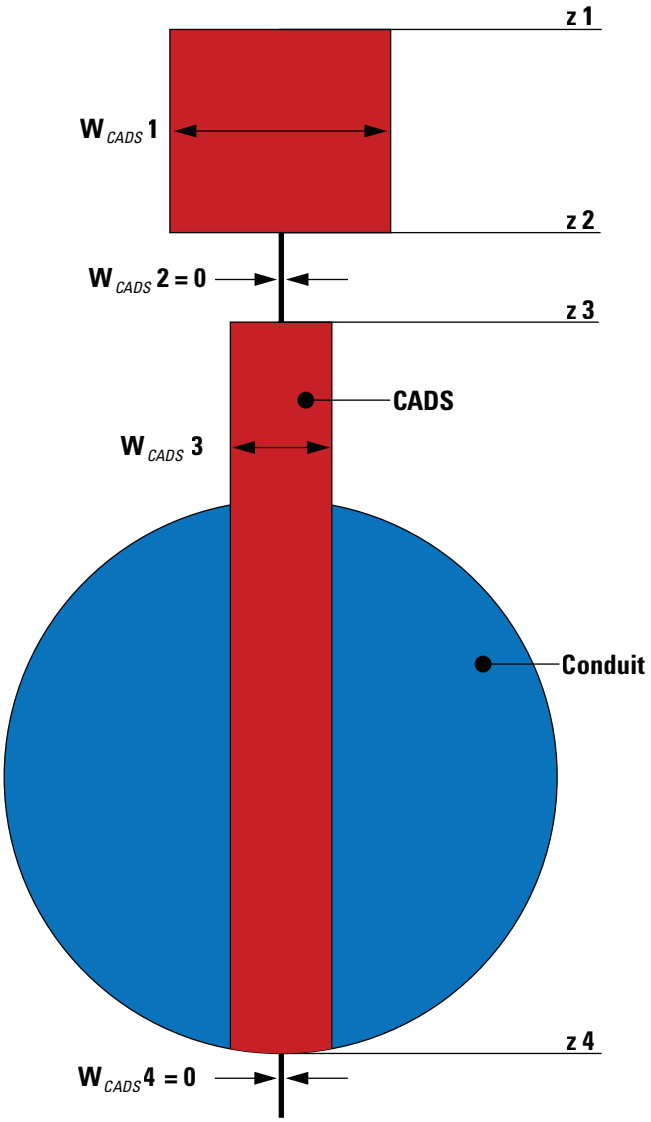

Figure 7.6. Conceptual diagram for multi-layer conduit-associated drainable storage (CADSML) package.

CADS Recharge

The CADS recharge allows defining the percentage of diffuse areal recharge that is directly routed into CADS. By definition, the CADS heads are equal to conduit heads, and therefore, CADS recharge results in immediate flow from the CADS-associated node into tubes. In subsequent iterations, this additional tube discharge causes head variations in conduits (and CADS). By implementing CADS as described, CADS recharge is hydraulically equal to conduit recharge.

Partially Filled Pipe Storage (PFPS)

The CFP2 was modified from the previous version to account for flow through partially filled pipes. If pipes are partially filled (for example, pipe bottom is less than head and head is less than pipe top), the CFP2 Mode 1 corrects the flow computation to apply appropriately to partially filled pipes (Shoemaker and others, 2008). The water volume coming from and going to the pipe storage is computed for tracking budget terms. This newly developed feature for the CFP2 Mode 1 improves representation of pipe storage in the water budget (that is, PFPS is part of the active flow system resulting in additional discharge). Figure 7.7 is a conceptual sketch of the PFPS implementation.

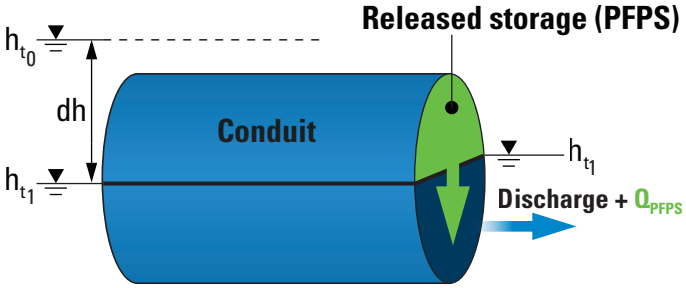

Figure 7.7. Conceptual implementation of partially filled pipe storage (PFPS). Drawdown, dh, equals the change in hydraulic head during the time step (t_0 until t_1); the outflow discharge at t_1 is the sum of conduit inflow and the flow rate, Q_{PFPS}, of released storage as the pipe transitions from filled to partially filled.

The flow rate in and out, or change in storage (Q), in PFPS is estimated similarly as in CADS (see the "Conduit Associated Drainable Storage" section):

$$Q_{PFPS} = \frac{V_{t2} - V_{t0}}{\Delta t} \tag{7.9}$$

where

V_t is the volume at time, t, and
V_{t0} is the initial volume at the start of the time step.

Unlike in CADS, the volume is no longer a linear function of head (h). The finite difference of volume resulting from head change can be computed, however, as follows:

$$V_{t1} - V_{t0} = f\left(h_{t1}\right) - f\left(h_{t0}\right) = \frac{f\left(h_{t1}^{kiter-1}\right) - f\left(h_{t0}\right)}{h_{t1}^{kiter-1} - h_{t0}}\left(h_{t1}^{kiter} - h_{t0}\right) \tag{7.10}$$

where

$h_{t1}^{kiter-1}$ is the hydraulic head in the previous iteration at time, t;
h_{t1}^{kiter} is the hydraulic head in the current iteration; and
h_{t0} is the hydraulic head in the previous iteration at the start of the time step.

The functional behavior of $V = f(h)$ is described by Shoemaker and others (2008, p. 8) and is beyond the scope of this document. Please note that PFPS does not include dry pipes; if the head falls below the conduit base, the pipe is no longer partly full, and PFPS is not active.

It should be noted that CFP2 Mode 1 is not designed to compute karst hydraulics in partially filled conduits. The free-surface flow processes in partially filled pipes can result in unsteady flow with considerable effects due to inertial forces and momentum. The steady-state approach implemented in CFP Mode 1 neglects dynamic processes (for example, water released from PFPS is immediately part of the active flow system, resulting in an immediate change of discharge); therefore, flow computation with PFPS considered can be unstable for some situations with too much water release from PFPS. For instance, large head changes or large conduit diameters can result in increasing discharge ($Q_{overall} + Q_{PFPS}$), increasing heads, filled conduits, and, therefore, $Q_{PFPS} = 0$.

References Cited

Bauer, S., Liedl, R., and Sauter, M., 2005, Modeling the influence of epikarst evolution on karst aquifer genesis—A time-variant recharge boundary condition for joint karst-epikarst development: Water Resources Research, v. 41, no. 9, 12 p., https://doi.org/10.1029/2004wr003321.

Fleury, P., Maréchal, J.-C., and Ladouche, B., 2013, Karst flash-flood forecasting in the city of Nîmes (southern France): Engineering Geology, v. 164, p. 26–35. https://doi.org/10.1016/j.enggeo.2013.06.007.

Király, L., 1997, Modelling karst aquifers by the combined discrete channel and continuum approach, 6th Conference on limestone hydrology and fissured aquifers: Université de Franche-Comté, Sciences et Technique de l'Environment, La Chaux-de-Fonds, p. 1–26.

Liedl, R., Sauter, M., Hückinghaus, D., Clemens, T., and Teutsch, G., 2003, Simulation of the development of karst aquifers using a coupled continuum pipe flow model: Water Resources Research, v. 39, no. 3, 11 p., https://doi.org/10.1029/2001WR001206.

Mangin, A., 1994, Karst hydrogeology, *in* Stanford, J., Gibert, J., and Danielopol, D., eds., Ground-water ecology: San Diego, Calif., Academic Press, p. 43–67.

Maréchal, J.-C., Ladouche, B., Dörfliger, N., and Lachassagne, P., 2008, Interpretation of pumping tests in a mixed flow karst system: Water Resources Research, v. 44, no. 5, 18 p., https://doi.org/10.1029/2007WR006288.

Shoemaker, W.B., Kuniansky, E.L., Birk, S., Bauer, S., and Swain, E.D., 2008, Documentation of a conduit flow process (CFP) for MODFLOW-2005: U.S. Geological Survey Techniques and Methods Book, Chapter A24, 50 p., https://pubs.usgs.gov/tm/tm6a24/pdf/tm6-A24.pdf.